Published online July 15, 2004

3760–3770 *Nucleic Acids Research, 2004, Vol. 32, No. 12*
doi:10.1093/nar/gkh672

Exploration of the conserved A+C wobble pair within the ribosomal peptidyl transferase center using affinity purified mutant ribosomes

Ashley Eversole Hesslein, Vladimir I. Katunin[1], Malte Beringer[2], Anne B. Kosek, Marina V. Rodnina[2] and Scott A. Strobel*

Yale University, Department of Molecular Biophysics and Biochemistry, 260 Whitney Avenue, New Haven, CT 06520 8114, USA, [1]Petersburg Nuclear Physics Institute, Gatchina 188355, Russia and [2]Institute of Physical Biochemistry, University of Witten/Herdecke, Stockumer Strasse 10, 58448 Witten, Germany

Received April 14, 2004; Revised May 19, 2004; Accepted June 8, 2004

ABSTRACT

Protein synthesis in the ribosome's large subunit occurs within an active site comprised exclusively of RNA. Mutational studies of rRNA active site residues could provide valuable insight into the mechanism of peptide bond formation, but many of these mutations cause a dominant lethal phenotype, which prevents production of the homogeneous mutant ribosomes needed for analysis. We report a general method to affinity purify *in vivo* assembled 50S ribosomal subunits containing lethal active site mutations via a U1A protein-binding tag inserted onto the 23S rRNA. The expected pH-dependent formation of the A2450+C2063 wobble pair has made it a potential candidate for the pH-dependent conformational change that occurs within the ribosomal active site. Using this approach, the active site A2450+C2063 pair was mutated to the isosteric, but pH-independent, G2450•U2063 wobble pair, and 50S subunits containing the mutations were affinity purified. The G•U mutation caused the adjacent A2451 to become hyper-reactive to dimethylsulfate (DMS) modification in a pH-independent manner. Furthermore, the G•U mutation decreased both the rate of peptide bond formation and the affinity of the post-translocation complex for puromycin. The reaction rate (k_{pep}) was reduced ~200-fold for both puromycin and the natural aminoacyl-tRNA A-site substrate. The mutations also substantially altered the pH dependence of the reaction. Mutation of this base pair has significant deleterious effects upon peptidyl transferase activity, but because G•U mutation disrupts several tertiary contacts with the wobble pair, the assignment of A2450 as the active site residue with the neutral pK_a important for the peptidyl transferase reaction cannot be fully supported or excluded based upon these data.

INTRODUCTION

All cells synthesize polypeptides within the ribosome, a large ribonucleoprotein particle. The 50S large ribosomal subunit catalyzes peptide bond formation within the peptidyl transferase center (PTC), an active site comprised exclusively of RNA (1,2). The reaction substrates are an aminoacyl-tRNA and a peptidyl-tRNA, which bind to the A site and P site of the ribosome, respectively (3). The PT reaction involves aminolysis of the ester linkage in the peptidyl-tRNA by the aminoacyl-tRNA α-amino group.

Within the past few years, extensive structural information about the ribosome has been generated, providing a wealth of new insight regarding the chemical details of this biologically ancient enzyme (1,2,4–6). These structural studies confirm years of biochemical data, while demonstrating that the PT reaction is catalyzed within the 23S rRNA. The observation that the ribosome catalyzes peptide bond formation using an RNA active site led to the obvious question: how does the rRNA contribute to peptide bond catalysis? It has already been established that nucleotides within the rRNA are responsible for correctly binding and positioning the 3′-CCA ends of the A-site and P-site tRNA for substrate reactivity (7–11), but is there further catalytic involvement by rRNA nucleotides in the PT reaction?

The pH dependence of the PT reaction potentially provided useful information about ribosomal catalysis. Early kinetic experiments demonstrated that the reaction rate increases with increasing pH, revealing an apparent reaction pK_a of 7.2–7.6 (12–14). This was originally thought to be titration of an active site histidine residue, but the absence of amino acid residues in the active site have forced this interpretation to be reconsidered. Recent measurements involving a rapid factor dependent PT assay demonstrated that there are two reaction pK_a's, and thus titration of two groups contributes to the

*To whom correspondence should be addressed. Tel: +1 203 432 9772; Fax: +1 203 432 5767; Email: strobel@csb.yale.edu
Present address:
A.E. Hesslein, Process and Technology Development, Bayer HealthCare, Berkeley, CA 94107, USA

reaction (15). One pK_a of 6.9 was attributed to deprotonation of the small molecule A-site substrate puromycin (Pmn), whereas the second pK_a of ~7.5 was attributed to deprotonation of a ribosomal residue.

The chemical identity of the ribosomal group with a 7.5 pK_a remains unknown, though two possibilities have been suggested previously (15). (i) The titratable group is the N3 position of A2451, which acts as a general base to deprotonate the α-amino group of the A-site tRNA. To serve this role, the pK_a of A2451 N3 would have to be perturbed by as much as 6 pH units. Although this possibility cannot be ruled out, the charge relay mechanism that was originally proposed to achieve such a perturbation is not consistent with subsequent experimental data (1,16). (ii) The titratable group is the N1 of A2450, which is protonated within the pH dependent and highly conserved non-canonical A2450+C2063 wobble pair adjacent to the site of peptide bond formation (15,17). N1 protonation allows it to serve as a hydrogen bond donor to the O2 of cytosine (Figure 1A).

A2450 N1 protonation is consistent with the orientation of A2450 and C2063 in the 50S crystal structure solved at acidic pH (pH 5.8) (2). The pK_a of the adenosine N1 in a model A+C pair is perturbed toward neutrality (pKa = 6.0–6.5) as determined by using NMR (18). This N1 perturbation corresponds to a pK_a shift of ~2–3 pH units, but the local environment of the PT active site could perturb the pK_a still higher. In this scenario, the protonated A+C wobble conformation would be the less active form of the ribosome, whereas the deprotonated form would more efficiently catalyze the reaction (15). At pHs below neutrality, A2450 would be protonated and the base pair would be intact; however, at elevated pHs the A2450 would be deprotonated, and the base pair would be destabilized. The A+C wobble could act as a pH-dependent molecular switch between the fully active and the less active forms of PTC.

In order to test the role of the A2450+C2063 wobble pair in the PT reaction, it would be useful to site specifically mutate these nucleotides. The G•U wobble pair is isosteric with an A+C pair, but pH independent (Figure 1A). However, because the ribosome is essential for cellular viability, mutations in critical active site residues often cause lethal or dominant lethal phenotypes, which make conventional mutagenesis difficult (19).

Several approaches have been developed to biochemically analyze dominant lethal ribosomal mutants. One approach is to express the rRNA mutant in the background of a second mutation that confers antibiotic resistance. The mixed ribosomal population is incubated with the antibiotic, which inactivates the wild-type (wt) ribosomes in the population, but leaves the mutant ribosomes unaffected (20,21). However, antibiotics typically reduce activity only ~100-fold (22), which leaves a relatively small signal-to-noise ratio for mutant analysis. Any mutation that slows reactivity by an amount approaching 100-fold would be uninformative in such an assay. A second approach is to analyze the kinetics of peptide bond formation in a mixed ribosome population, and then deconvolute the rates of the two populations (15). Although this approach

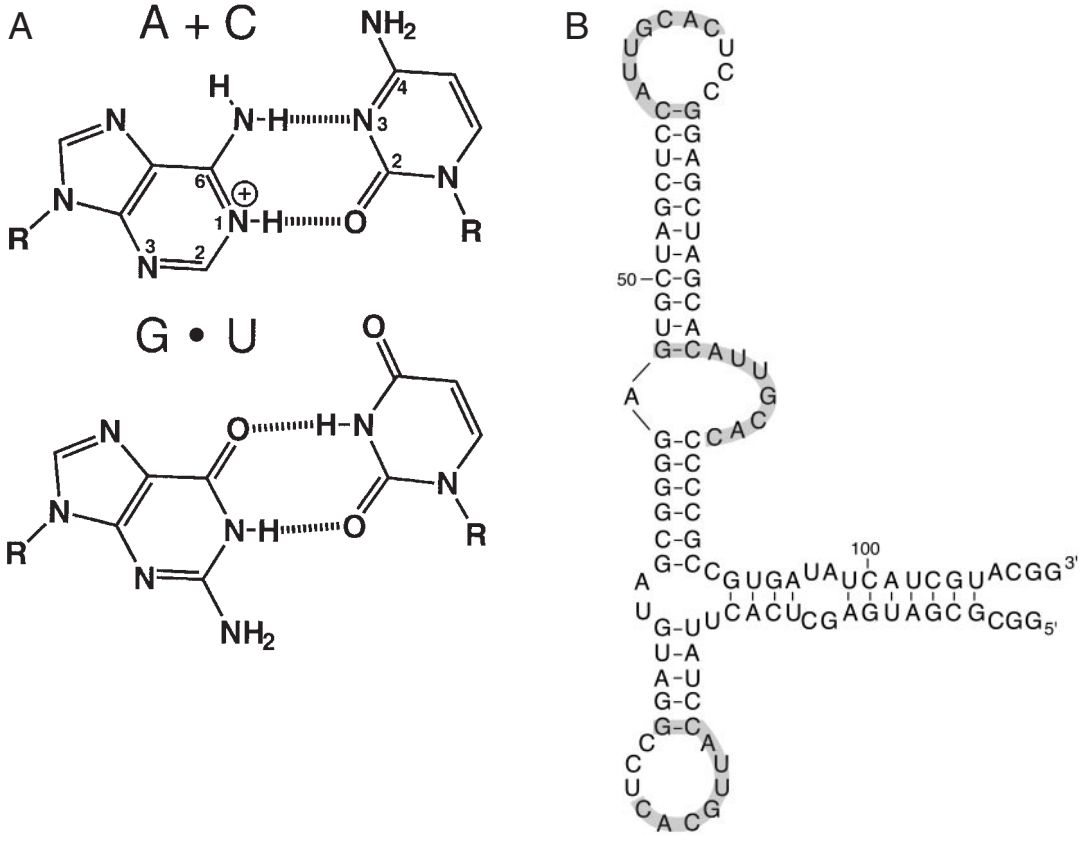

Figure 1. (**A**) Schematic representation of an A+C (upper panel) and a G•U wobble pair (lower panel). In this study the A2450+C2063 pair is mutated to a G•U pair. (**B**) Diagram of the U3X-tag inserted into the 23S rRNA for affinity purification. The three U1A-binding sites are delineated in gray.

was successfully performed on an A2451U active site point mutant, separation of the two rates was extremely laborious. Ribosomal reconstitution using *in vitro* transcribed 23S rRNA and total 50S ribosomal proteins provides a third means to generate mutant ribosomes (23–25). However, the reconstitution is notoriously inefficient and the resultant ribosomes are significantly less active than the *in vivo* assembled particles.

Here, we report an alternative approach to generate homogeneous ribosomes with dominant lethal point mutations in the 23S rRNA. In this system mutated rRNA is inducibly expressed and assembled into 50S subunits *in vivo*, and the mutant ribosomes are purified from wt subunits using a protein affinity tag on the RNA (Figure 1B). The RNA tag is a modified U1A-binding site that is recognized by His_6-tagged U1A protein which is co-expressed with the mutant rRNA. Affinity purification produced 50S particles in sufficient yields and purity for use in chemical footprinting and PT reaction analysis. We utilized this purification system to test the effect of the pH-independent A2450G•C2063U mutant wobble base pair on peptide bond formation.

MATERIALS AND METHODS

Expression and purification of His_6U1A

His_6U1A was expressed from a pET15 vector (Qiagen) and purified on Ni^{2+}-nitrilotriacetate (Ni-NTA) agarose (Qiagen) according to the manufacturer's protocol. Following column purification, the eluant was dialyzed twice against 1 litre of 20 mM Tris–HCl (pH 7.5), 100 mM NaCl, 1 mM DTT and 20% glycerol. The protein was loaded onto a hydroxyapatite column using an Akta FPLC (Pharmacia), eluted with 0.5 M ammonium sulfate and dialyzed against 1 litre of 20 mM Tris–HCl (pH 7.5), 100 mM KCl, 1 mM DTT, 0.1 mM EDTA and 10% glycerol, and stored at −20°C.

Construction of the U3X-tagged rRNA plasmid

A multi-step procedure was used to insert the U3X-tag at various positions in the rrnB operon of plasmid pLK35. A new set of AscI/XhoI/BsiWI restriction sites were inserted at four target sites (see Results) in 23S rRNA using QuickChange(tm) (Stratagene). None of these restriction enzymes cleaves pLK35. The modified pLK35 plasmids were digested with AscI and BsiWI, gel purified and CIP treated. The annealed and phosphorylated oligonucleotides corresponding to the U3X insert were ligated to the cut plasmid. Transformed colonies were screened for loss of the XhoI site and gain of an EcoRV site. The plasmids were confirmed by sequence analysis (Yale University, Keck facility). The final sequence of the U3X-tag is shown in Figure 1B. A single U1A-binding site (U1X) of sequence CCCTGACCCGAATTCCATTGCACTCCGGAGTTTGGGTCCTGAA was inserted using the QuickChange protocol.

Purification of 50S ribosomal subunits

Escherichia coli 50S ribosomal subunits were purified from pop2136 cells as described in (26) with the following modifications. Spin times were adjusted for a Beckman Ti70 rotor. Following the first wash step, the ribosomes were resuspended in 20 mM Tris–HCl (pH 7.6), 0.5 M NH_4Cl, 1.5 mM magnesium acetate, 0.5 mM EDTA and 7 mM 2-mercaptoethanol, and incubated at 4°C for 4 h to dissociate the subunits. The subsequent wash step was done with this low magnesium buffer. Mixed 30S and 50S particles were stored at 4°C until the Ni-NTA purification step. We found that ribosomes purified with the buffer and salt conditions reported here were more active in peptidyl transfer than ribosomes prepared according to (27).

Homogeneous U3X-tagged 50S particles for use in small-scale affinity purifications were isolated from MC250 cells by zonal centrifugation in a Beckman Ti 14 rotor on a 10–40% sucrose gradient (450 ml) in 20 mM Tris–HCl (pH 7.6), 60 mM NH_4Cl, 5.2 mM magnesium acetate, 0.25 mM EDTA and 3.0 mM 2-mercaptoethanol (45 000 r.p.m. for 4 h 15 min at 4°C). 50S subunits were stored at −80°C in 70 mM NH_4Cl, 30 mM KCl, 7 mM $MgCl_2$, 1 mM DTT, 0.5 mM EDTA and 50 mM Tris–HCl (pH 7.6).

Small-scale affinity purification of U3X-tagged ribosomes

His_6U1A protein (500 pmol) was mixed with pre-equilibrated Ni-NTA agarose (from 40 µl of 50% slurry) in 100 µl 1× PD for 30 min at 4°C. The beads were centrifuged gently for 2 min at 4°C, excess U1A was removed, and the beads were washed twice in 1× PD buffer (50 mM Tris–HCl (pH 7.6) 70 mM NH_4Cl, 30 mM KCl, 10 mM $MgCl_2$, 5 mM imidazole, 10 µg/ml tRNA and 10 µg/ml heparin). Ribosomes were added (167 pmol) in a 100 µl volume. After 1 h of rocking at 4°C, unbound ribosomes were removed, the beads were washed twice with 1× PD, and the His_6U1A-bound ribosomes were eluted in 1× EB (same as 1× PD except it also contained 200 mM imidazole and lacked tRNA and heparin).

Construction of a His_6U1A plasmid for co-expression with rRNA

Plasmid PPU used to co-express the His_6U1A protein was constructed as follows. The ~3.9 kb pACYC184 (New England Biolabs) BamHI/HindIII fragment, containing the chloramphenicol resistance marker and the ColE1 compatibility group origin of replication, was ligated to the 1.7 kb BamHI/HindIII digestion product of pAS1 (Clontech), which contained the lambda P_L promoter. The His_6U1A coding sequence was PCR amplified with primers containing a BamHI site at both ends and cloned into the BamHI site in the pACYC184/pAS1 plasmid. The orientation and sequence of the final product was confirmed by sequence analysis (Yale University, Keck facility). P_L is controlled by the lambda phage cI857 repressor, which is integrated into the genome of pop2136 cells. Incubation at 42°C inactivates the repressor, leading to gene expression. The ColE1 origin is compatible with the pLK35-derived plasmids used to express the rRNA.

Large-scale induction and affinity purification of U3X-tagged ribosomes

rRNA transcription was induced by growing pop2136 cells containing plasmid pLK35-U3X-B at 30°C in ampicillin (Amp) until they reached an OD_{600} of 0.1. The cells were grown for an additional 2–3 h at 42°C until they reached a final OD_{600} between 0.8 and 1.0. Cells co-induced for rRNA and His_6U1A expression were grown using the same approach

except both Amp and chloramphenicol were included in the media. 50S ribosomal subunits were purified from these cells as described above.

The heterogeneous ribosomal subunits were mixed with Ni-NTA agarose in a 50 ml conical tube. An aliquot of 1 ml of Ni-NTA agarose (50:50 slurry) was added per 40 nmol of crude ribosomes, and 7.5× vol of 1× PD per ml of bead. The mixture was rocked in the cold room for 20 min. The slurry was poured over an empty column, and the flow-through was collected and re-poured over the column. The column was washed in 20× column volumes of 1× PD, and eluted in 25 ml of 1× EB. The eluted ribosomes were pelleted for 3.5 h at 60 000 r.p.m. in a Ti70 ultracentrifuge rotor (Beckman). Purified ribosomes were resuspended in ribosome storage buffer (see above) and stored at −80°C.

Primer extension assay to measure purification efficiency

23S rRNA was isolated from ribosomes by phenol/chloroform extraction. A ^{32}P-radiolabeled primer complementary to the 23S rRNA sequence (1226 and 1206) was annealed downstream of the U3X insertion site in 100 mM KCl, 50 mM Tris–HCl, pH 8.5. The primer was extended with AMV Reverse Transcriptase (AMV-RT Roche) for 30 min at 42°C in manufacturer supplied buffer supplemented with 1 mM each dCTP, dATP, dTTP and ddGTP. Products were resolved on a 20% 19:1 acrylamide gel. For the U3X-tagged rRNA, the first incorporated G is four nucleotides from the end of the primer, whereas the first G is seven nucleotides from the primer in the untagged 23S rRNA. Relative band intensities for the +4 and the +7 products were quantified on a STORM PhosphorImager (Molecular Dynamics) and ImageQuant software. rRNA purity was calculated by comparing the ratio of the +4 band intensity (tagged) to the total intensity of the +4 and +7 bands.

70S PT kinetic analysis and post-translocation complex formation

Preparation of the 30S subunits, tRNAs, initiation and elongation factors was performed as described previously (15,16,26). 30S subunits were reactivated by heating for 1 h at 37°C in buffer 50 mM Tris–HCl, 20 mM Bis–Tris (pH 7.2) 30 mM KCl, 70 mM NH_4Cl and 20 mM $MgCl_2$. The 70S initiation complex was prepared in buffer A (50 mM Tris–HCl, 20 mM Bis–Tris (pH 7.2) 30 mM KCl, 70 mM NH_4Cl and 7 mM $MgCl_2$) by incubating wt 30S ribosomes with 50S subunits (1 μM each), MFT-mRNA (4 μM; coding for fMet-PheThr) and f[^{3}H]Met-tRNA^{fMet} (1.5 μM; 3000–4000 d.p.m./pmol) in the presence of initiation factors 1, 2 and 3 (1.5 μM each) for 15 min at 37°C. Complexes were purified and concentrated by centrifugation through 1.1 M sucrose cushions in buffer A at 259 000×*g* for 2 h (Sorvall M120GX). Ternary complex EF-Tu·GTP·[^{14}C]Phe-tRNA^{Phe} was prepared by incubating EF-Tu (2.4 μM) with GTP (1 mM), phosphoenolpyruvate (3 mM) and pyruvate kinase (0.1 μg/ml) for 15 min at 37°C after which Phe-tRNA^{Phe} (1.2 μM) was added. The rate of fMetPhe formation was measured upon mixing equal volumes (14 μl) of initiation (0.2 μM) and ternary complexes (1.2 μM) in a quench-flow KinTek apparatus at 37°C. The reaction products released from f[^{3}H]MetPhe-tRNA^{Phe} by alkaline hydrolysis in 0.5 M KOH (for 30 min at 37°C), separated by reverse phase high-performance liquid chromatography (RP-HPLC), and quantified using double-label radioactivity counting.

Post-translocation complexes were prepared by incubating EF-Tu·GTP·[^{14}C]Phe-tRNA^{Phe} (1 μM; 1000 d.p.m./pmol) with initiation complexes (1 μM) for 10 min at 20°C. Peptide bond formation resulted in ribosomes carrying deacylated tRNA^{fMet} in the P-site and f[^{3}H]Met[^{14}C]Phe-tRNA^{Phe} in the A-site. Upon incubation (5 min) with EF-G (0.02 μM) and GTP (1 mM), f[^{3}H]Met[^{14}C]Phe-tRNA^{Phe} was translocated to the P-site. Complexes were purified by ultracentrifugation as described above. Quench-flow assays were performed at 37°C by mixing equal volumes of ribosome (0.2 μM) and Pmn (as indicated) solutions and analyzed as described above.

A2451 reactivity to dimethylsulfate

Ribosomes were reacted with dimethylsulfate (DMS) as described in (17) except the reaction was carried out in 50 mM buffer (MES, pH 6.0, HEPES, pH 6.5–8.5), 150 mM KCl and 15 mM $MgCl_2$. All ribosomes were activated at 42°C for 10 min in reaction buffer prior to incubation with DMS. The primer used for this analysis was 2493 (28).

RESULTS

Design and placement of an RNA affinity tag

Affinity purification of 50S ribosomes containing 23S rRNA mutations requires that the tag be placed on the rRNA. We selected an affinity tag recognized by the eukaryotic protein splicing factor U1A for the following reasons: (i) U1A is a low molecular weight protein (14 kDa), so its presence should be minimally disruptive to the ribosome provided that the RNA tag is properly positioned; (ii) U1A binds the 11 nt consensus RNA sequence with high specificity and affinity (29,30); (iii) U1A is a eukaryotic protein, so there should be low background binding to *E.coli* RNAs; and (iv) the recombinant U1A is efficiently expressed in *E.coli* with good yields and high purity (29,31). Based upon these considerations, we designed a ~100 nt RNA tag (U3X) containing three tandem copies of the U1A consensus-binding site (Figure 1B). The ability of the U3X affinity tag to bind U1A was confirmed by gel-shift analysis with recombinant His_6U1A protein (data not shown).

The site of U3X-tag insertion within the 23S rRNA was selected based upon phylogenetic and *in vivo* complementation analysis. To function in affinity purification, the RNA tag must be solvent-accessible, it must not disrupt rRNA secondary and tertiary structures, and it must not disrupt major functions of the ribosome, such as subunit association, factor binding or ribosome assembly. Three potential tag insertion sites were selected in helix 9 (termed A), helix 46 (termed B) and helix 54 (termed C) by examining where 23S rRNA sequence expansions had been tolerated during evolution (32). All three sites showed length variation >100 nt. Thus, all of these locations could theoretically accommodate an insertion of the size of ~100 nt U3X-tag. A fourth tag insertion site in helix 98 (termed D) was chosen based upon experimental precedence of extending helix 98 (33). We inserted a single U1A-binding site, U1X, at this position because the

naturally occurring sequence variation ranged only 0–19 nt. The theoretical compatibility of each site was visually confirmed by inspection of the *Haloarcula marismortui* 50S subunit structure (2).

The compatibility of the U3X insertions was tested in an *E.coli* strain (MC250) where the plasmid encoded U3X-tagged rRNA was the only rRNA operon available to the cell (34). The strain lacks all seven chromosomal rRNA operons and thus needs to be supplemented with rRNA from a plasmid. We transformed the MC250 cells with a plasmid containing the rrnB operon (pLK35) with the U3X-tag sequence inserted at positions A, B or C, or the U1X-tag sequence inserted at position D. Cell growth was well supported by rRNA production from the wt plasmid, but the U3X insertion at positions A and C, and U1X insertion at position D substantially interfered with cell growth (data not shown). The effect upon position D insertion was surprising given that this site was tolerant of a tRNA insertion in a previous report (33). Insertion at site B was the only tagged rRNA construct that permitted ribosomal function at levels similar to wt. This construct (pLK35-U3X-B) was used for all subsequent analysis.

Inducible expression of rRNA mutants in *E.coli*

The goal in developing this system was the expression and purification of dominant lethal 23S rRNA mutants. In addition to the tag, this required an inducible expression system in which mutated 23S rRNA could be produced in the background of chromosomal 23S rRNA transcription. We selected the inducible expression system under the control of a chromosomally encoded temperature-sensitive lambda repressor in *E.coli* strain pop2136 (35). Cells were initially grown at 30°C, where the mutant rRNA was not expressed, and then shifted to 42°C to induce rRNA expression prior to lysing the cells and purifying the 50S ribosomal subunits.

The U3X-tagged rRNA served as a marker of mutant ribosome expression in this mixed population of wt and mutant ribosomes. The U3X-tag sequence on the rRNA was confirmed by primer extension. After 2–3 h of induction at 42°C, ~50% of total cellular rRNA and 20% of the fully assembled 50S subunits contained the U3X-tagged 23S rRNA (data not shown). These values were comparable to previously reported expression levels of rRNA from the P_L promoter (20,34,36). Thus, this brief induction period was sufficient to achieve reasonably high levels of tagged ribosome expression.

Affinity purification of tagged ribosomes

Small-scale trial experiments demonstrated that U3X-tagged ribosomes could be retained and eluted on a Ni-NTA column. Ribosomal proteins were retained on the column only when the 23S rRNA was U3X-tagged, as evidenced by SDS–PAGE analysis (Figure 2A, compare lanes 7 and 11). Bound ribosomes were eluted by adding imidazole, which disrupts the His_6UIA interaction with Ni-NTA.

Although the trial experiments with purified His_6U1A were successful, generating a sufficient quantity of His_6U1A protein for large-scale ribosomal affinity purification would immediately become a limiting factor. To circumvent the His_6U1A purification steps, we designed a two plasmid system that utilized temperature-sensitive co-expression of both the U3X-tagged rRNA and the His_6U1A protein. Plasmid PPU was constructed with the His_6U1A protein expressed under the control of the temperature-sensitive lambda repressor and a ColE1 compatible origin of replication (for details see Materials and methods). Co-expression of rRNA from the pLK35-U3X-B plasmid and His_6U1A protein from the PPU plasmid did not slow pop2136 cell growth significantly (data not shown). We anticipated that the His_6U1A would bind the U3X-tag *in vivo*, and remain bound during the subsequent purification. This would obviate the need for independent purification of the U1A protein. In addition, U1A binding *in vivo* could help protect the U3X-tag from ribonuclease degradation damage that may occur during the expression and purification process. Improved longevity of the RNA tag could lead to improved yields of mutant 50S ribosomes.

A large-scale purification of U3X-tagged ribosomes from a mixed population was performed to test the yield and purity of the affinity purification process. Separation of the purified ribosomes by ultracentrifugation in a sucrose gradient showed that the eluted fraction contained exclusively 50S subunits (data not shown). The yield of purified U3X-tagged ribosomes was ~4% of the total ribosomes in the cell at the time of lysis. The eluted fraction was tested for purity by primer extension analysis. Greater than 95% of the 50S ribosomal subunits in the purified fraction contained a U3X-tag (Figure 2B). This is likely to underestimate the purity because the analysis gives an estimate of 3% tagged even when the ribosomes were 100% untagged (Figure 2B, lane 2).

Characterization of the affinity purified ribosomes

Several assays were used to determine whether the rate of peptide bond formation was affected by the U3X-tag or the affinity purification process. The first activity assay measured how well affinity purified tagged ribosomes initiated translation. Untagged 50S subunits or purified U3X-tagged 50S subunits were incubated with f[^{3}H]Met-tRNA^{fMet}, 30S subunits, mRNA, initiation factors and GTP. Binding of f[^{3}H]Met-tRNA^{fMet} to the 70S particle was measured by nitrocellulose filtration. Within the 15 min incubation, 73% of the wt ribosomes and 61% of the tagged ribosomes bound to the fMet-tRNA^{fmet}. This suggests that initiation activity was not significantly affected by the tag or the purification protocol.

The ability of affinity purified ribosomes to form a dipeptide was tested by mixing initiation complexes containing a P-site f[^{3}H]Met-tRNA^{fMet} with [^{14}C]Phe-tRNA^{Phe}, which had been pre-incubated with EF-Tu, GTP, phosphoenolpyruvate and pyruvate kinase (16). HPLC analysis of the product measured the extent of dipeptide formed by unpurified or affinity purified ribosomes in this single-turnover reaction. The untagged ribosomes reacted to a 75% end point, while the affinity purified ribosomes reacted to an end point of 60%. Thus, the U3X-tag and the affinity purification process had only minimal effects on the extent of dipeptide formation.

Next, we characterized the U3X ribosomes for tripeptide formation. In this reaction the fMetPhe-tRNA^{Phe} is translocated to the P-site by EF-G. This post-translocation complex is incubated with Pmn, a small molecule mimic of the

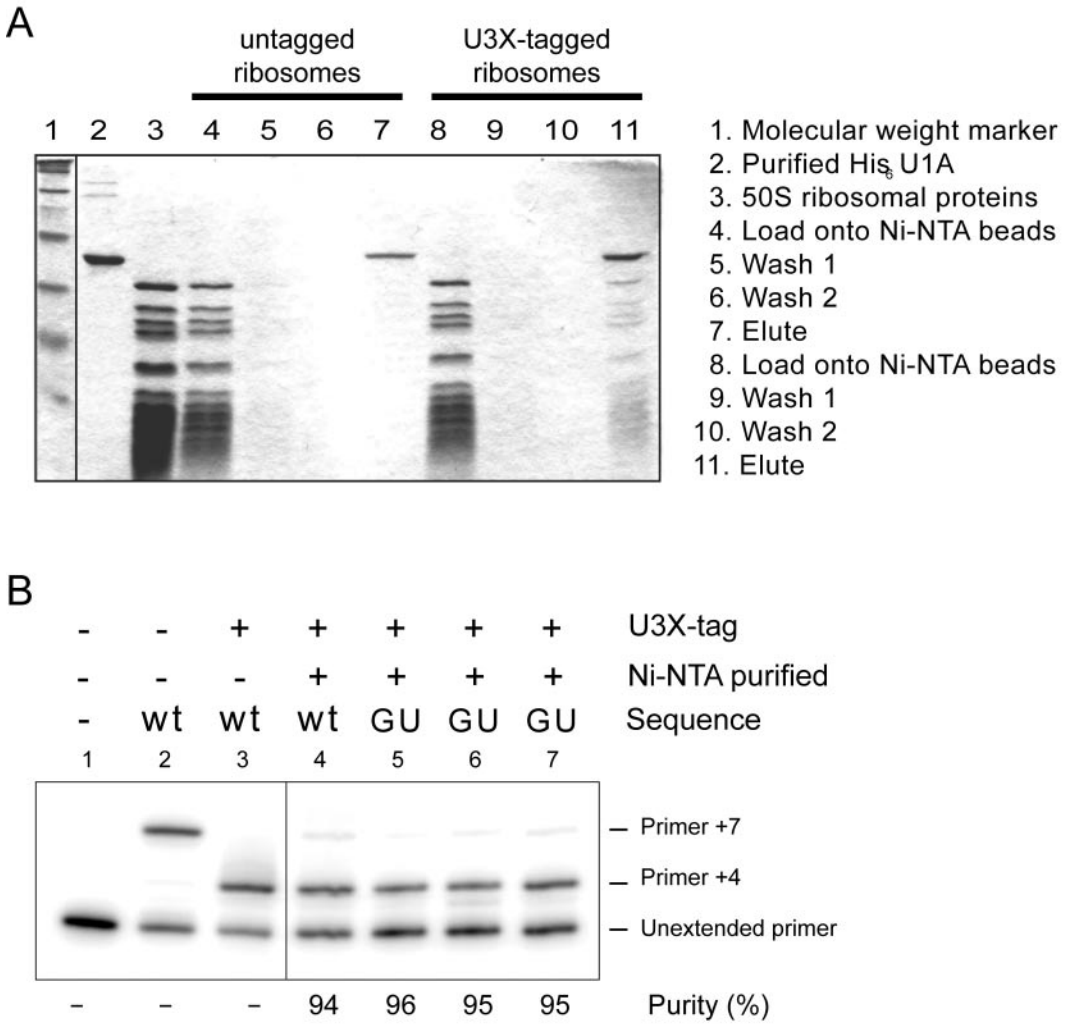

Figure 2. Affinity purification of U3X-tagged 50S ribosomes. (**A**) Selective retention of U3X-tagged 50S ribosomes by His_6U1A protein. Ribosomes or ribosomes containing a U3X-tag were affinity purified by incubation with Ni-NTA and His_6U1A protein. Aliquots of the batch purification process were analyzed by SDS–PAGE, as indicated, and stained with Coomassie Blue. (**B**) Analysis of ribosome purity by primer extension. Lane 1, no template. Lane 2, untagged rRNA control. Lane 3, homogeneous U3X-tagged rRNA control. Lanes 4–6, affinity purified 23S rRNA from U3X-tagged wt or G•U wobble mutant (GU) ribosomes. Lanes 5 and 6 are from two independent large-scale purifications of G•U ribosomes. Lane 7, G•U mutant 23S rRNA from ribosomes in the translocation complex.

aminoacyl-tRNA. Pmn reaction with the fMetPhe-tRNA results in the tripeptide fMetPhePmn (16). The reaction end point for the untagged ribosomes was 59%, whereas 33% of the U3X-tagged ribosomes reacted. This suggests that the inactive fraction in the tagged ribosomes was slightly larger than the untagged, possibly resulting from the purification process. In both cases, the majority of the reaction was completed by the first time point (10 s).

The rate of the PT reaction was measured under conditions in which the chemical step is expected to be rate limiting (15) (Figure 3A). The untagged ribosomes reacted at a rate of $12\ s^{-1}$, which was 2-fold faster than the rate of the affinity purified ribosomes ($6\ s^{-1}$) (pH 7.5, 37°C). Thus, there is a slight deleterious effect of tagging and affinity purifying the ribosomes, but it is a modest effect that can be readily controlled for. Thus, in all of the cellular viability and ribosomal reactivity assays, tag insertion and affinity purification has no more than 2-fold effect.

Mutation and kinetic characterization of the active site A2450G•C2063U wobble pair mutation

The U1A tag affinity purification system was used to investigate the active site A2450G•C2063U wobble pair mutation in an effort to test if the A2450 N1 is the functional group in the PTC with a pK_a of 7.5. As discussed above, the A2450 N1 is likely to have a perturbed pK_a based upon the wobble conformation of the equivalent A2450+C2063 base pair in the *H.marismortui* 50S crystal structure (A2485+C2104 pair in *H.marismortui*) and the NMR studies show that the adenosine N1 pK_a is perturbed in A+C wobble pairs (18). A G•U pair is isosteric with an A+C wobble pair, but it is pH independent (Figure 1A). Therefore, we set out to test how mutation of the A+C pair to a G•U would affect the pH dependence of the active site.

The A2450G•C2063U mutation, like many active site mutations, has a dominant lethal phenotype. Ribosomes with the G•U mutation could not support growth when provided as the

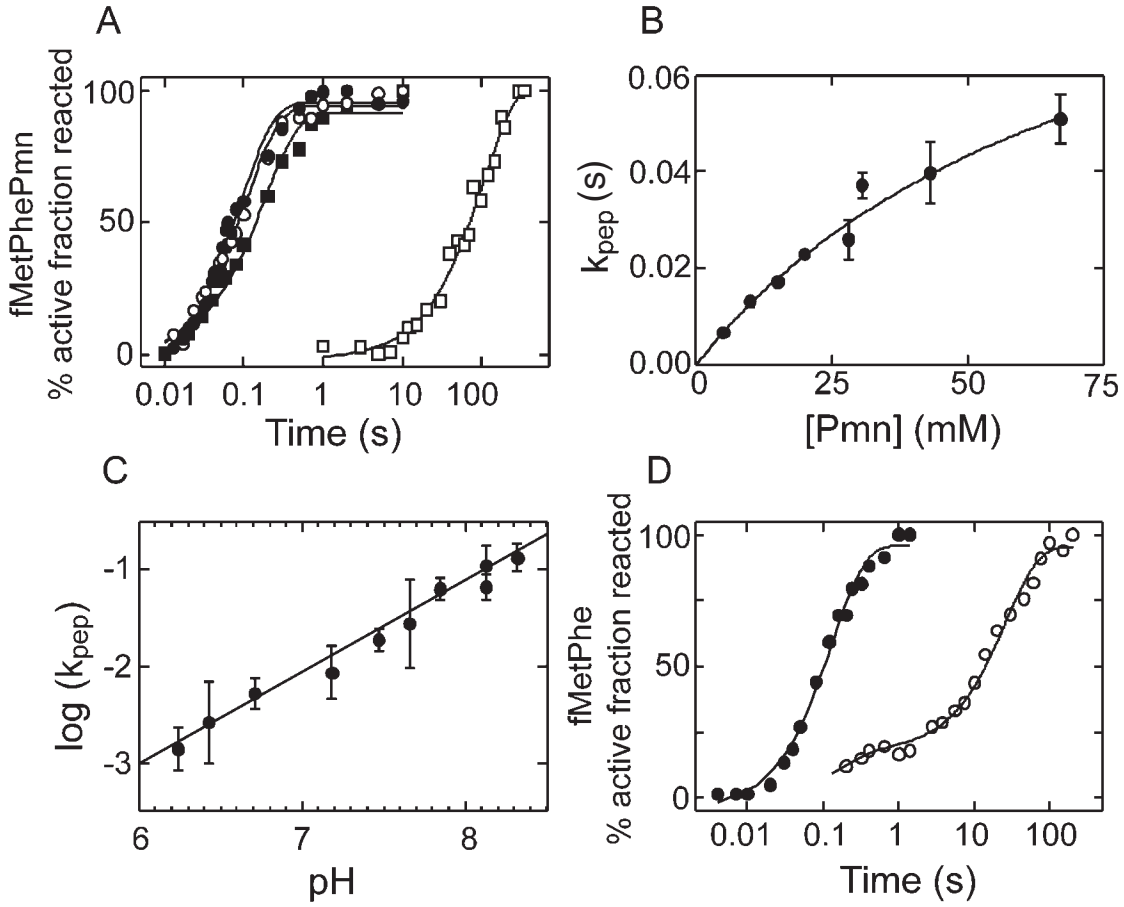

Figure 3. Kinetic analysis of G•U mutant ribosomes. (**A**) Rate of tripeptide formation in the reaction between fMetPhe-tRNA^{Phe} and Pmn. The extent of reaction is plotted as a function of time for wt 50S ribosomes prepared using standard protocols from pop2136 (closed circles) or MRE600 (open circles) cells, U3X-tagged wt 50S ribosomes (closed squares) and U3X-tagged G•U mutant ribosomes (open squares) prepared by affinity purification. The reaction was normalized to the final amplitudes of the extent of tripeptide formation. (**B**) Concentration dependence of Pmn reaction (37°C, pH 7.2). Further increase in concentration was not feasible due to limited solubility of Pmn. (**C**) pH dependence of the G2450•U2063 affinity purified mutant ribosomes at 10 mM Pmn (37°C). The reaction rate is plotted versus the pH in the range 6.2–8.3. (**D**) Rate of dipeptide formation in the reaction between fMet-tRNA^{fMet} and Phe-tRNA^{Phe}. The extent of reaction is plotted as a function of time for wt 50S ribosomes (closed circles) and U3X-tagged G•U mutant ribosomes (open circles) prepared by affinity purification. The reaction is normalized to the final amplitudes of the extent of dipeptide formation.

only source of ribosomes in MC250 cells (data not shown). Furthermore, expression of the mutant interfered with growth when co-expressed with wt ribosomes in pop2136 cells (data not shown). Therefore, in order to biochemically assay ribosomes with this mutation, it was necessary that they should be affinity purified.

The A2450G•C2063U point mutations were introduced into the U3X-tagged rRNA construct pLK35-U3X-B. The resulting plasmid was co-transformed with the U1A protein expression plasmid into pop2136 cells. Tagged mutant ribosomes and the His_6U1A protein were co-induced at 42°C and the ribosomes affinity purified to a level ⩾95% pure (Figure 2B, lanes 5 and 6). The yield after purification was ∼4–7% of all ribosomes for wt, and ∼4–5% of all ribosomes for G•U mutants. Mutation of the active site did not cause significant reduction in cell growth during the 2–3 h induction.

The mutant ribosomes were analyzed using the same PT assays outlined above. Initiation was not adversely affected by the mutation. A total of 55% of the mutant ribosomes bound fMet-tRNA compared to 61% for purified wt ribosomes. The end point of dipeptide formation was largely unaffected by the mutant, in that there was 50% product formation after 10 min at 20°C compared to 60% for purified wt ribosomes, therefore the dipeptide formation occurred with near quantitative yields. The fMetPhe-tRNAs were translocated to the P-site, and the amount of U3X-tagged rRNA in the post-translocation complex measured by primer extension. The percentage purity of the rRNA was unchanged (95%; Figure 2B, lane 7) indicating that there was no selection against the G2450•U2063 mutant in the post-translocation complex. This complex was then assayed for peptide bond formation upon Pmn addition. The reaction end points were unaffected by the G•U mutant (33% for purified G•U wobble ribosomes and 27% for purified wt ribosomes), but the reaction rates were substantially different. The wt affinity purified ribosomes reacted at a rate of 6 s^{-1}, while the G•U wobble mutants reacted at only 0.01 s^{-1} (10 mM Pmn, 37°C, pH 7.2; Figure 3A).

The observed decrease in the rate of Pmn reaction on the mutant ribosomes may be due to a slower rate of catalysis or to a weaker binding of Pmn. To distinguish between the two possibilities, we measured the dependence of k_{pep} on Pmn

concentration (Figure 3B). The affinity of Pmn to the ribosomes was strongly decreased by the G•U wobble mutation to a K_d of ~80 mM compared to 3 mM measured with the wt ribosomes (15). The rate constant of peptide bond formation extrapolated to Pmn saturation was 0.1 s^{-1} (pH 7.2), 180-fold slower than on the wt ribosomes at the same pH.

pH dependence of G•U mutant ribosomes

In wt ribosomes, the slope of the reaction rate as a function of pH is 1.5, which has been interpreted to mean that the reaction involves at least two ionizable groups (15). One of these is the α-amino group of Pmn, while the second is an ionizable group in the ribosome. The PT reaction rates of the G•U wobble ribosomes were measured as a function of pH and plotted (Figure 3C). The measurements were carried out at limiting concentration of Pmn (10 mM), because saturating concentrations cannot be achieved due to limited solubility. The slope of the pH dependence of rate is 0.95, a value that would be consistent with the removal of an ionizing A+C base pair in the active site; however, there is no inflection in the pH dependence between pH 5 and 8, which is unexpected. Although several explanations are possible, it appears that the pK_a of Pmn is no longer a limiting factor in the assay. Most likely, the loss of the Pmn pK_a appears to result from the inability to saturate the A-site with Pmn, as the pH dependence under the k_{cat}/K_M conditions may reveal ionizing groups involved in Pmn binding, rather than in catalysis.

Peptide bond formation with the natural A-site substrate

Given that the mutant ribosomes appeared capable of forming dipeptide but showed a large loss of reactivity with Pmn, we set out to determine if the inactivity resulted from the use of a small molecule tRNA mimic rather than full tRNAs. The rate of dipeptide formation was measured between fMet-tRNA^{fMet} and Phe-tRNA^{Phe} for the wt and mutant ribosomes (Figure 3B). The wt ribosomes produced fMetPhe-tRNA^{Phe} at a rate of 7.5 ± 0.5 s^{-1}, while the rate of the mutant ribosomes was 0.04 ± 0.003 s^{-1}, a 200-fold rate reduction at a saturating concentration of the ternary complex (1.2 μM). Thus, the reduced activity of these ribosomes does not appear to be an artifact of the Pmn assay. The rate of peptide bond formation is substantially reduced even with full tRNA substrates in the A-site and P-site.

Chemical footprinting of the rRNA active site in G•U wobble mutants

Given the substantial rate reduction and change in reaction pH dependence, we next asked if the mutant caused a conformational change in the PTC that could be detected by chemical footprinting. We assayed for DMS alkylation at A2451, a residue whose DMS reactivity in *E.coli* has been argued to reflect an inactive PTC conformation (37). There is a striking DMS-dependent reverse transcriptase stop at A2451 in the G•U mutant ribosomes (Figure 4). The intensity of the A2451 reactivity was substantially greater than that has been observed previously in the wt ribosomes (37,38), and the reactivity was pH independent (Figure 4). A2451 alkylation was independent of any of the standard methods used to alter the PTC conformational state (37). The extent of methylation remained constant between 50S subunits tested directly after purification and subunits that had been 'activated' by incubating at 42°C for 10 min. Furthermore, there was no change in subunits 'inactivated' by dialysis to remove potassium and sodium ions, and subunits that were 'inactivated' and subsequently 'reactivated' by adding 150 mM KCl and incubating at 42°C. These data suggest that the G•U mutant ribosomes are locked in an inactive and pH-independent conformation.

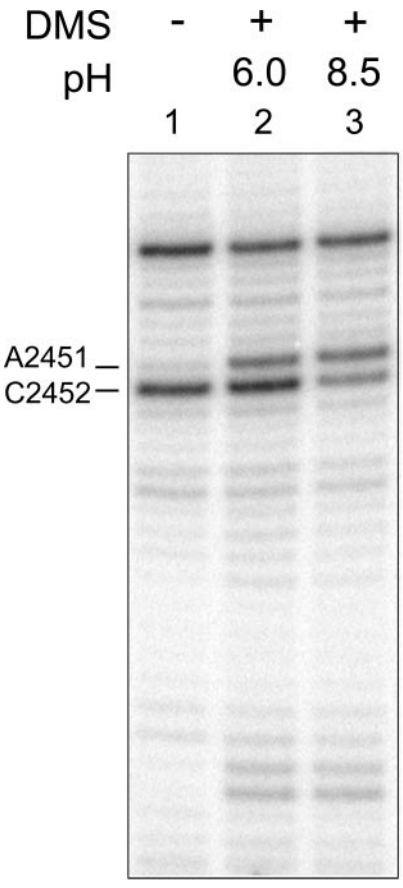

Figure 4. DMS modification of G2450•U2063 mutant ribosomes as a function of pH. Ribosomes were incubated at pH 6.0 or 8.5 in the absence (−) or presence (+) of DMS. The 23S rRNA was purified and used as a template for primer extension of a radiolabeled primer. The resulting products were separated by denaturing gel electrophoresis. RT stops at nucleotides C2452 and A2451 are indicated.

DISCUSSION

Detailed knowledge of how RNA catalyzes peptide bond would provide valuable insight into how this ancient enzyme functions. Biochemical analysis of ribosomal mutants is impaired by the fact that many active site mutations have a dominant lethal phenotype. We set out to develop a robust system for producing *in vivo* assembled mutant ribosomes in order to facilitate biochemical characterization of dominant lethal mutations. The approach involved introducing a U1A affinity tag into the 23S rRNA and co-expressing the mutant ribosomes with a His_6-tagged form of the U1A protein. A His_6-tagged U1A protein binds both to Ni-NTA agarose beads and the tagged ribosomes, making it possible to purify

tagged ribosomes away from cellular expressed wt ribosomes. The tag insertion at A1205 and affinity purification were minimally disruptive to the PT reaction. Mutant ribosomes are greater than 95% pure after one affinity-purification step. Ribosomal yields following purification were sufficient for footprinting experiments and kinetic analysis of peptide bond formation, and were successfully used to examine ribosome reaction rates.

In the course of this study two other groups reported an affinity purification approach to isolate large ribosomal subunits with dominant lethal 23S rRNA mutations (39,40). Leonov *et al*. (39) introduced a streptavidin aptamer sequence into helix 25 and used this tag to affinity purify ribosomes with a G2655C mutation that affects translocation. Youngman *et al*. (40) inserted an MS2 protein-binding site into helix 98. They used this system to extensively characterize mutations at four active site positions for their effect on the PT and peptide release reaction rates. They did not explore mutations at A2450+C2063, and they did not investigate the pH dependence of the mutant ribosome reactivity.

The PTC undergoes a conformational change with a pK_a of ~7.5 and the PT reaction is promoted by deprotonation of an active site group with the same pK_a (15,17). The two most commonly suggested candidates for the titratable active site group are the N3 of A2451 and the protonated A2450+C2063 wobble pair (2,15,17,38). A2451 was localized to the reaction center repeatedly by using biochemical footprinting studies (9,41,42). It was reported to have a DMS profile in *E.coli* that correlates with the pK_a of PT, though subsequent studies showed the apparent pH-dependent reactivity must correspond to a conformational change (17,38). Mutation of A2451 to U altered the reaction pK_a as assayed in a mixed ribosomal population (15), though the possibility that this was an indirect effect resulting from an active site conformational change cannot be excluded. The biochemical data on A2451 leaves open the possibility that a different residue contains the ionizable group in the active site. For this reason, we used the affinity purification method to characterize the A2450G• C2063U wobble pair mutant.

In the *H.marismortui* 50S crystal structure determined at pH 5.8, the A2450+C2063 (A2485+C2104 in *H.marismortui*) pair is in a wobble configuration (2) (Figure 5). Although protons are not visible in this structure, the arrangement of the two nucleotides and the pH of the solution is consistent with A2450 (A2485) N1 protonation. One model we have suggested is that deprotonation of this group at near neutral pH could induce a conformational change in the PTC that promotes reactivity. The G•U wobble pair is isosteric with the A+C wobble, but its formation is pH independent in the neutral pH range (Figure 1A). Assuming there are no other changes in the active site resulting from the mutations, the G•U would stabilize the wobble pair, which would keep the active site in the less active conformation and reduce the pH dependence of the reaction. This hypothesis was explored with affinity purified A2450G+C2063U mutant 50S ribosomes using both chemical reactivity and enzyme kinetics assays.

The results of the A2451 DMS reactivity experiments on the G•U mutant ribosomes are somewhat unexpected. In the *H.marismortui* 50S crystal structure, the N1 of A2451 (A2486) is hydrogen bonded to G2061 (G2102) and is not solvent accessible (Figure 5). 50S *E.coli* ribosomes in an 'activated' conformation (induced by heating to 42°C) are notably unreactive to DMS at A2451 (37). Therefore, DMS reactivity at A2451, which occurs at the N1 position, indicates that the residue is solvent exposed and in a conformation different than that observed in the crystal structure. In the context of the G2450•U2063 mutation, A2451 becomes substantially more reactive to DMS modification, which is in contrast to the expectation that the G•U mutation would stabilize the conformation observed in the crystal structure. However, as expected from the experimental design, the reactivity is pH independent. Furthermore, A2451 is insensitive to any efforts

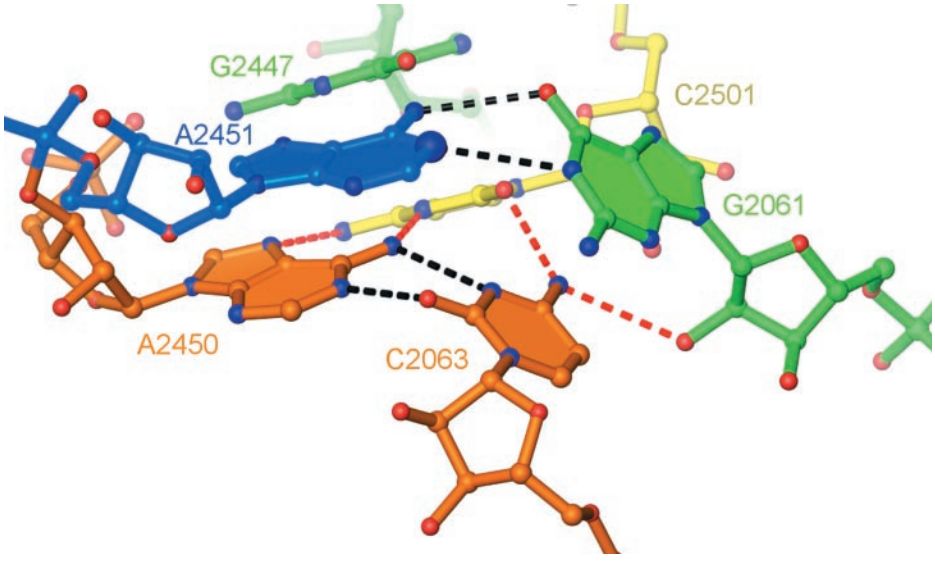

Figure 5. Structure of conserved residues within the 23S rRNA active site from the *H.marismortui* 50S subunit crystal structure (2). The A2450+C2063 wobble pair (*E.coli* numbering) is shown in orange, A2451 is shown in blue, G2061 and G2447 are shown in green and C2501 is in yellow. The N1 of A2451 that reacts with DMS is shown as an enlarged sphere. The hydrogen bonds between A2450+C2063 that are likely to be disrupted by mutation to a G•U pair are shown in red. This includes interactions within the A2450+C2063-C2501 triple, as well as the G2061-A2451-G2447 triple stacked above it.

to 'activate' or 'inactivate' the ribosomes. Thus, these data suggest that mutation to G•U results in a pH-insensitive active site conformation, but the conformation is not the one observed in the low pH 50S crystal structure.

The affinity purified G•U mutant ribosomes were also analyzed for effects on peptide bond formation. Mutation had no significant effect prior to formation of the post-translocation complex, including initiation and translocation, but the G•U mutation reduced the rate of peptide bond formation with both Pmn and aminoacyl-tRNA by ~200-fold. The magnitude of the Pmn effect was similar to that of the A2451U mutation, as assayed in a mixed ribosome population (15). Although the pH dependence of the residual reactivity changed substantially, it did not follow a pattern consistent with any previously defined model of the reaction mechanism. The substantial reduction in the rate of peptide bond formation is consistent with the hypothesis that A2451 DMS reactivity is indicative of an inactive conformation.

The contradictory nature of the data suggests that the G2450•U2063 mutation is not isomorphous with the A+C pair within the confines of the tightly folded PTC. The A2450+C2063 pair is part of a base triple that includes C2501 (*E.coli* numbering) (Figure 5). This triple stacks with a second triple (G2447•A2451•G2061) that includes the active site A2451. Although the conformation of the isolated G•U wobble pair is predicted to be isosteric with an A+C pair, this is unlikely to be true of the entire C2501• A2450+C2063 base triple. At least two of the three hydrogen bonds to C2501 are lost in the G•U mutation (A2450 N6-C2501 N3 and C2063 N4-C2501 O2). For both hydrogen bonds the G•U mutation would cause lone pairs of electrons to be juxtaposed. Unfortunately, there is no combination of the naturally occurring nucleosides that would produce a pH-independent base triple that is isosteric with C2501• A2450+C2063. C2501 also makes a tertiary contact to the 2′-OH of G2061 (Figure 5), a hydrogen bond that appears to connect the two base triples. It is possible that displacement of U2063 away from C2501 would in turn displace G2061 away from A2451. This would explain the hypersensitivity of A2451 to DMS modification. In addition to these effects, the G•U mutation introduces an amino group into the active site at position 2450, which may explain why the effect on peptide bond formation is so large. As a result of these considerations, the assignment of A2450 as the active site residue with the neutral pK_a important for the PT reaction cannot be supported or completely excluded based upon these data on the G2450•U2063 mutation. However, it is clear that mutation of this base pair has a significant deleterious effect upon PT activity.

We have successfully developed a gentle non-disruptive affinity purification method for isolation of *in vivo* assembled lethal mutant 50S ribosomes. The relative simplicity of the co-expression and purification method will make it possible to biochemically explore other mechanistic hypotheses regarding the role of rRNA in peptide bond synthesis.

ACKNOWLEDGEMENTS

We thank Peter Adams for U1A purification, Dmytro Rodnin for 30S ribosome preparations, and Astrid Böhm, Petra Striebeck and Carmen Schillings for expert technical assistance. Thanks to Albert Dahlberg, Michael O'Conner, Nigel Grindley and Catherine Joyce for bacterial expression plasmids, strains and advice. This work was supported by NIH grant GM54839 to S.A.S. and by the Deutsche Forschungsgemeinschaft (M.V.R. and V.I.K.), the Alfried Krupp von Bohlen und Halbach-Stiftung (M.V.R.), Fonds der Chemischer Industrie (M.V.R.), the Russian Foundation for Basic Research (V.I.K.), and the International Bureau of BMBF (V.I.K.), and HSF-DAAD Grant to S.A.S. and M.V.R.

REFERENCES

1. Nissen,P., Hansen,J., Ban,N., Moore,P.B. and Steitz,T.A. (2000) The structural basis of ribosome activity in peptide bond synthesis. *Science*, **289**, 920–930.
2. Ban,N., Nissen,P., Hansen,J., Moore,P.B. and Steitz,T.A. (2000) The complete atomic structure of the large ribosomal subunit at 2.4 Å resolution. *Science*, **289**, 905–920.
3. Green,R. and Noller,H.F. (1997) Ribosomes and translation. *Annu. Rev. Biochem.*, **66**, 679–716.
4. Yusupov,M.M., Yusupova,G.Z., Baucom,A., Lieberman,K., Earnest,T.N., Cate,J.H. and Noller,H.F. (2001) Crystal structure of the ribosome at 5.5 Å resolution. *Science*, **292**, 883–896.
5. Harms,J., Schluenzen,F., Zarivach,R., Bashan,A., Gat,S., Agmon,I., Bartels,H., Franceschi,F. and Yonath,A. (2001) High resolution structure of the large ribosomal subunit from a mesophilic eubacterium *Cell*, **107**, 679–688.
6. Bashan,A., Agmon,I., Zarivach,R., Schluenzen,F., Harms,J., Berisio,R., Bartels,H., Franceschi,F., Auerbach,T., Hansen,H.A. *et al*. (2003) Structural basis of the ribosomal machinery for peptide bond formation, translocation, and nascent chain progression. *Mol. Cell*, **11**, 91–102.
7. Lieberman,K.R. and Dahlberg,A.E. (1994) The importance of conserved nucleotides of 23S ribosomal RNA and transfer RNA in ribosome catalyzed peptide bond formation. *J. Biol. Chem.*, **269**, 16163–16169.
8. Samaha,R.R., Green,R. and Noller,H.F. (1995) A base pair between tRNA and 23S rRNA in the peptidyl transferase centre of the ribosome. *Nature*, **377**, 309–314.
9. Bocchetta,M., Xiong,L. and Mankin,A.S. (1998) 23S rRNA positions essential for tRNA binding in ribosomal functional sites. *Proc. Natl Acad. Sci. USA*, **95**, 3525–3530.
10. Kim,D.F. and Green,R. (1999) Base-pairing between 23S rRNA and tRNA in the ribosomal A site. *Mol. Cell*, **4**, 859–864.
11. Bocchetta,M., Xiong,L., Shah,S. and Mankin,A.S. (2001) Interactions between 23S rRNA and tRNA in the ribosomal E site. *RNA*, **7**, 54–63.
12. Fahnestock,S., Neumann,H., Shashoua,V. and Rich,A. (1970) Ribosome-catalyzed ester formation. *Biochemistry*, **9**, 2477–2483.
13. Pestka,S. (1972) Peptidyl-puromycin synthesis on polyribosomes from *Escherichia coli*. *Proc. Natl Acad. Sci. USA*, **69**, 624–628.
14. Maden,B. and Monro,R. (1968) Ribosome-catalyzed peptidyl transfer. Effects of cations and pH value. *Eur. J. Biochem.*, **6**, 309–316.
15. Katunin,V.I., Muth,G.W., Strobel,S.A., Wintermeyer,W. and Rodnina,M.V. (2002) Important contribution to catalysis of peptide bond formation by a single ionizing group within the ribosome. *Mol. Cell*, **10**, 339–346.
16. Beringer,M., Adio,S., Wintermeyer,W. and Rodnina,M. (2003) The G2447A mutation does not affect ionization of a ribosomal group taking part in peptide bond formation. *RNA*, **9**, 919–922.
17. Muth,G.W., Chen,L., Kosek,A.B. and Strobel,S.A. (2001) pH-dependent conformational flexibility within the ribosomal peptidyl transferase center. *RNA*, **7**, 1403–1415.
18. Cai,Z. and Tinoco,I.,Jr (1996) Solution structure of loop A from the hairpin ribozyme from tobacco ringspot virus satellite. *Biochemistry*, **35**, 6026–6036.
19. Triman,K.L. (1999) Mutational analysis of 23S ribosomal RNA structure and function in *Escherichia coli*. *Adv. Genet.*, **41**, 157–195.
20. Porse,B.T. and Garrett,R.A. (1995) Mapping important nucleotides in the peptidyl transferase centre of 23S rRNA using a random mutagenesis approach. *J. Mol. Biol.*, **249**, 1–10.

21. Nierhaus,K.H., Beyer,D., Dabrowski,M., Schafer,M.A., Spahn,C.M., Wadzack,J., Bittner,J.U., Burkhardt,N., Diedrich,G., Junemann,R. *et al*. (1995) The elongating ribosome: structural and functional aspects. *Biochem. Cell. Biol*., **73**, 1011–1021.
22. Thompson,J., Kim,D.F., O'Connor,M., Lieberman,K.R., Bayfield,M.A., Gregory,S.T., Green,R., Noller,H.F. and Dahlberg,A.E. (2001) Analysis of mutations at residues A2451 and G2447 of 23S rRNA in the peptidyl transferase active site of the 50S ribosomal subunit. *Proc. Natl Acad. Sci. USA*, **98**, 9002–9007.
23. Green,R. and Noller,H.F. (1999) Reconstitution of functional 50S ribosomes from *in vitro* transcripts of *Bacillus stearothermophilus* 23S rRNA. *Biochemistry*, **38**, 1772–1779.
24. Khaitovich,P., Tenson,T., Kloss,P. and Mankin,A.S. (1999) Reconstitution of functionally active *Thermus aquaticus* large ribosomal subunits with *in vitro*-transcribed rRNA. *Biochemistry*, **38**, 1780–1788.
25. Semrad,K. and Green,R. (2002) Osmolytes stimulate the reconstitution of functional 50S ribosomes from *in vitro* transcripts of *Escherichia coli* 23 s rRNA. *RNA*, **8**, 401–411.
26. Rodnina,M.V. and Wintermeyer,W. (1995) GTP consumption of elongation factor Tu during translation of heteropolymeric mRNAs. *Proc. Natl Acad. Sci. USA*, **92**, 1945–1949.
27. Rheinberger,H.-J., Geigenmuller,U., Wedde,M. and Nierhaus,K.H. (1988) Parameters for the preparation of *Escherichia coli* ribosomes and ribosomal subunits active in tRNA binding. *Methods Enzymol*., **164**, 658–670.
28. Stern,S., Moazed,D. and Noller,H.F. (1988) Sructural analysis of RNA using chemical and enzymatic probing monitored by primer extension. *Methods Enzymol*., **164**, 481–489.
29. van Gelder,C.W.G., Gunderson,S.I., Jansen,E.J., Boelens,W.C., Polycarpou-Schwarz,M., Mattaj,I.W. and van Venrooij,W.J. (1993) A complex secondary structure in U1A pre-mRNA that binds two molecules of U1A protein is required for regulation of polyadenylation. *EMBO J*., **12**, 5191–5200.
30. Nagai,K., Oubridge,C., Ito,N., Jessen,T.H., Avis,J. and Evans,P. (1995) Crystal structure of the U1A spliceosomal protein complexed with its cognate RNA hairpin. *Nucleic Acids Symp. Ser*., **34**, 1–2.
31. Ferre-D′Amare,A.R. and Doudna,J.A. (2000) Crystallization and structure determination of a hepatitis delta virus ribozyme: use of the RNA-binding protein U1A as a crystallization module. *J. Mol. Biol*., **295**, 541–556.
32. Cannone,J.J., Subramanian,S., Schnare,M.N., Collett,J.R., D'Souza,L.M., Du,Y., Feng,B., Lin,N., Madabusi,L.V., Muller,K.M. *et al*. (2002) The Comparative RNA Web (CRW) site: an online database of comparative sequence and structure information for ribosomal, intron, and other RNAs. *BMC Bioinformatics*, **3**, 15.
33. Spahn,C.M.T., Grassucci,R.A., Penczek,P. and Frank,J. (1999) Direct three-dimensional localization and positive identification of RNA helices within the ribosome by means of genetic tagging and cryo-electron microscopy. *Structure*, **7**, 1567–1573.
34. O'Connor,M., Lee,W.M., Mankad,A., Squires,C.L. and Dahlberg,A.E. (2001) Mutagenesis of the peptidyltransferase center of 23S rRNA: the invariant U2449 is dispensable. *Nucleic Acids Res*., **29**, 710–715.
35. Gregory,S.T., Brunelli,C.A., Lodmell,J.S., O'Connor,M. and Dahlberg,A.E. (1998) Genetic selection of rRNA mutations. *Methods Mol. Biol*., **77**, 271–281.
36. Rosendahl,G., Hansen,L.H. and Douthwaite,S. (1995) Pseudoknot in Domain II of 23 S rRNA is essential for ribosome function. *J. Mol. Biol*., **249**, 59–68.
37. Bayfield,M.A., Dahlberg,A.E., Schulmeister,U., Dorner,S. and Barta,A. (2001) A conformational change in the ribosomal peptidyl transferase center upon active/inactive transition. *Proc. Natl Acad. Sci. USA*, **98**, 10096–10101.
38. Muth,G.W., Ortoleva-Donnelly,L. and Strobel,S.A. (2000) A single adenosine with a neutral p*K*a in the ribosomal peptidyl transferase center. *Science*, **289**, 947–950.
39. Leonov,A.A., Sergiev,P.V., Bogdanov,A.A., Brimacombe,R. and Dontsova,O.A. (2003) Affinity purification of ribosomes with a lethal G2655C mutation in 23S rRNA that affects the translocation. *J. Biol. Chem*., **278**, 25664–25670.
40. Youngman,E.M., Brunelle,J.L., Kochaniak,A.B. and Green,R. (2004) The active site of the ribosome is composed of two layers of conserved nucleotides with distinct roles in peptide bond formation and peptide release. *Cell*, **117**, 589–599.
41. Moazed,D. and Noller,H.F. (1989) Interaction of tRNA with 23S rRNA in the ribosomal A, P, and E sites. *Cell*, **57**, 585–597.
42. Moazed,D. and Noller,H.F. (1991) Sites of interaction of the CCA end of peptidyl-tRNA with 23S rRNA. *Proc. Natl Acad. Sci. USA*, **88**, 3725–3728.